Partition Function Zeros of Zeta-Urns

Condensed Matter Physics, 2024, Vol. 27, No. 3, 33601: 1–11
DOI: 10.5488/CMP.27.33601
http://www.icmp.lviv.ua/journal

CONDENSED MATTER PHYSICS

Partition function zeros of zeta-urns

P. Bialas [1], Z. Burda [2], D. A. Johnston [3*]

[1] Institute of Applied Computer Science, Jagiellonian University, ul. Lojasiewicza 11, 30-348 Kraków, Poland

[2] AGH University of Krakow, Faculty of Physics and Applied Computer Science, al. Mickiewicza 30, 30-059 Kraków, Poland

[3] School of Mathematical and Computer Sciences, Heriot-Watt University, Riccarton, Edinburgh EH14 4AS, UK

Received November 30, 2023, in final form January 24, 2024

We discuss the distribution of partition function zeros for the grand-canonical ensemble of the zeta-urn model, where tuning a single parameter can give a first or any higher order condensation transition. We compute the locus of zeros for finite-size systems and test scaling relations describing the accumulation of zeros near the critical point against theoretical predictions for both the first and higher order transition regimes.

Key words: *Lee-Yang and Fisher zeroes, critical exponents, first order phase transitions, second order phase transitions*

1. Introduction

In this paper we highlight the fact that a simple model of weighted partitions of indistinguishable particles into boxes, the zeta-urn model [1–3] in a grand-canonical ensemble where the number of *boxes* can fluctuate [4, 5], provides a useful illustrative example for exploring the finite size scaling of partition function zeros, since its finite size partition function is, at least in principle, exactly calculable and the order of its phase transition (condensation) may be tuned by varying a single parameter. The thermodynamic limit is also amenable to evaluation via saddle point methods.

In section 2 we first describe the formulation of the zeta-urn model in the canonical ensemble, since the partition function of the grand-canonical ensemble builds on the canonical partition function. The presence of a transition in the model is revealed by the breakdown of the saddle point approximation in the thermodynamic limit and its nature, a real space condensation [6–17], can be elucidated by explicitly evaluating the fraction of sites with q particles in a given configuration in finite size systems as the mean particle density is varied. We then discuss the thermodynamic limit in the grand-canonical ensemble and note that first or higher order transitions may be observed by tuning the power that appears in the weights for single box configurations. In section 3 we review some general features of partition function zeros [18–21, 23–30] and their finite size scaling for phase transitions of different orders [31], using both the density of zeros at a given system size and the scaling of the position of a given zero as the system size varies. In sections 4, 5 we investigate the application of these methods to studying the partition function zeros of the grand-canonical zeta-urn model. For $\beta > 1$, the model displays a phase transition and we discuss the first order and second/higher order regimes in subsections 5.1 and 5.2, respectively. The locus of zeros still displays interesting properties for values of β for which there is no phase transition (i.e., $\beta \leqslant 1$, including negative values) and we outline these in subsection 5.3. We close with a summary and brief discussion in section 6.

*Corresponding author: D.A.Johnston@hw.ac.uk.

2. Zeta-urn models

In the canonical ensemble, the partition function of the zeta-urn model, which is a particular case of a balls-in-boxes model, is defined by [1]

$$Z_{S,N} = \sum_{(s_1,\ldots,s_N)} w(s_1)\ldots w(s_N)\delta_{S-(s_1+\ldots+s_N)}, \tag{2.1}$$

with $w(s) = s^{-\beta}$ [1]. The name comes from the presence of the Riemann zeta function in the overall normalization and in the saddle point equations discussed below. The model describes power-law weighted distributions of S indistinguishable particles into N boxes. The s_i's denote the occupation numbers of the boxes $i = 1, \ldots, N$ and we take $s_i \geqslant 1$. The lowercase δ is the Kronecker delta.

A useful relation for evaluating $Z_{S,N}$ exactly follows from considering configurations with q balls in a given box. In that case the remaining $N-1$ boxes contain $S-q$ balls and are thus described by the partition function $Z_{S-q,N-1}$. This gives the recurrence relation

$$Z_{S,N} = \sum_{q=1}^{S-N+1} w(q) Z_{S-q,N-1} \tag{2.2}$$

for $S \geqslant N \geqslant q$, and $Z_{S,1} = w(S)$. The thermodynamic limit may be taken with both N and S being sent to infinity in a fixed ratio, i.e., $S \to \infty$, $\frac{N}{S} \to r$, where $r \in (0,1)$ is the reciprocal of the average particle density $\rho \equiv \frac{S}{N} = \frac{1}{r}$. The behaviour in the thermodynamic limit is encapsulated in a thermodynamic potential (a "free energy density" for the system)

$$\phi(r) = \lim_{S\to\infty} \frac{1}{S} \ln Z_{S,N} \tag{2.3}$$

at fixed r, that is, $\frac{N}{S} \to r \in (0,1)$. The potential $\phi(r)$ gives the rate of the asymptotic growth of the partition function as $S \to \infty$ at fixed r: $Z_{S,N} \propto \mathrm{e}^{S\phi(r)}$ and can be calculated using the saddle point method. The saddle point solution only holds for $r > r_{\mathrm{c}}$

$$r_{\mathrm{c}} = \frac{1}{\rho_c} = \frac{\zeta(\beta)}{\zeta(\beta-1)}. \tag{2.4}$$

To understand what is happening for $r < r_c$ (i.e., $\rho > \rho_c$), it is useful to look at the fraction of sites with q particles in a given configuration:

$$\pi(q) = \frac{1}{N} \sum_{i=1}^{N} \delta_{q-s_i}\ , \tag{2.5}$$

whose ensemble average is given by

$$\langle \pi(q) \rangle_{S,N} = \frac{w(q) Z_{S-q,N-1}}{Z_{S,N}}\ . \tag{2.6}$$

For $r < r_c$ ($\rho > \rho_c$), we can still use (2.2) to evaluate (2.6) exactly, even though the saddle point evaluation has broken down. If $\rho > \rho_c$, a peak appears in $\langle \pi(q) \rangle_{S,N}$ whose maximum is at $S(\rho - \rho_c)$ and whose sharpness increases with an increasing system size. This peak is a signal that an extensive fraction of the particles has condensed into a single box, which is a real space condensation [8, 9, 32–37]. For $\rho < \rho_c$, on the other hand, no box is distinguished and this phase is called "fluid".

It is possible to consider (amongst others) an ensemble with a variable number of boxes N controlled by a chemical potential μ. The corresponding partition function in this case is

$$Z_{S,\mu} = \sum_{N=1}^{S} \mathrm{e}^{-\mu N} Z_{S,N}, \tag{2.7}$$

where $Z_{S,N}$ is the canonical partition function defined in (2.1). With a slightly non-standard terminology, it has been customary to call (2.7) the "grand canonical" partition function [4].

In the thermodynamic limit, $S \to \infty$, the corresponding grand-canonical thermodynamic potential is defined as

$$\psi(\mu) = \lim_{S\to\infty} \frac{1}{S} \ln Z_{S,\mu}. \tag{2.8}$$

$\psi(\mu)$ is related to $\phi(r)$ by a Legendre-Fenchel transform

$$\psi(\mu) = \sup_{r\in[0,1]} \left(-\mu r + \phi(r)\right). \tag{2.9}$$

When the chemical potential exceeds the critical value, $\mu > \mu_c$, the saddle point equation breaks down and the average $r = r(\mu)$ drops to zero which, remembering r is an inverse density, is the grand-canonical version of the condensation transition in the model. For power-law weights, the critical value of the chemical potential is $\mu_c = \ln \zeta(\beta)$.

The singularities of grand-canonical potential $\psi(\mu)$ for power-law weights at the critical chemical potential $\mu_c = \ln \zeta(\beta)$ for $\beta > 1$ can be determined. The critical behaviour corresponds to $\mu_c - \mu \to 0^+$. It is found that the phase transition is first order for $\beta \in [2, +\infty)$ and higher order for $\beta \in (1, 2)$ [2, 4]. More precisely, for $\beta \in (1, 2)$ and for $\mu_c - \mu \to 0^+$

$$\psi''(\mu) \sim (\mu_c - \mu)^{-\lambda}, \tag{2.10}$$

where

$$\lambda = 2 - \frac{1}{\beta - 1}. \tag{2.11}$$

The symbol $\sim$ stands for the most singular part for $\mu_c - \mu \to 0^+$. We see that $\lambda \in [0, 1)$ for $\beta \in [3/2, 2)$, so the transition is second order in this range of β. More generally, it can be shown [2] that the transition is of n-th order for $\beta \in [1 + 1/n, 1 + 1/(n - 1))$. The transition disappears at $\beta = 1$ as the critical value of μ is pushed to infinity.

The zeta-urn model in the grand-canonical ensemble thus provides a model which displays both first order and continuous transitions of arbitrary order, as β is varied and whose partition function may be explicitly calculated for finite size systems by virtue of (2.2) and (2.7). In the remainder of the paper we exploit this to use it as a testing ground for examining the scaling properties of partition function zeros for transitions of various orders. Before doing this we set the scene with a discussion of the general properties of partition function zeros and their finite size scaling.

3. Partition function zeros

Regarding the partition function for a finite size system as a polynomial in some fugacity gives an appealing picture for understanding how singularities appear in the thermodynamic limit. For external field driven transitions, Lee and Yang [18, 19] made the key observation that if one considered complex fugacities, physical transitions appeared as the complex zeros of the partition function polynomial moved in to pinch the real positive axis in the complex fugacity plane in the thermodynamic limit. This point of view was then extended by Fisher to temperature driven transitions [20]. With a view to the application of this observation to the grand-canonical zeta-urn model discussed previously, we write the partition function for a system of size S, Z_S, as a polynomial in the fugacity, $z = \exp(-\mu)$

$$Z_S(z) = \prod_{j=1}^{S} \big(z - z_j(S)\big), \tag{3.1}$$

where j labels the zeros. Clearly, the two forms of the partition function (2.7) and (3.1) are equivalent $Z_{S,\mu} = Z_S(\mathrm{e}^{-\mu})$. One can define a thermodynamic potential

$$f_S(z) = \frac{1}{S} \ln Z_S(z) = \frac{1}{S} \sum_j \ln\big(z - z_j(S)\big), \tag{3.2}$$

Taking the limit as $S \to \infty$ leads to

$$f_\infty(z) = \int \mathrm{d}^2\xi \varrho(\xi) \ln(z - \xi), \tag{3.3}$$

where $\varrho(\xi)$ is the density of zeros on the complex plane. As $\ln|z - \xi|/2\pi$ is the Green function for the 2D Poisson equation, the last equation has an electrostatic analogy [21], with $\varrho(\xi)$ interpreted as charge density, and $\mathrm{Re}\, f_\infty(z)$ as electrostatic potential. For many statistical systems that undergo a phase transition, the distribution of zeros is known to display a very specific pattern. Near the critical point $x_\mathrm{c} = \mathrm{e}^{-\mu_\mathrm{c}}$ which is located on the positive real semi-axis, zeros lie on a one dimensional curve. This curve is symmetric with respect to the real axis because the partition function has real coefficients and as a consequence non-real zeros come in conjugate pairs. In the limit $S \to \infty$, the density of zeros on this curve near the critical point can be parameterized by a single parameter, which we take to be the imaginary part of zeros. For simplicity assume that the positive branch of this curve hits the real axis with a non-zero angle γ. Near the critical point the positive branch can be approximated by $\xi(y) = x_\mathrm{c} + cy + iy$ for $y < \epsilon \ll 1$, where $c = \cot(\gamma)$. The range ϵ is chosen as small as possible, so that higher powers of y in $\xi(y)$ can be neglected. For $\gamma = 0$ or π, that is when the curve is tangent to the real axis, the parameterisation of this curve by y is not optimal. However, this is not the case for the curves discussed below.

For a real argument $z = x$ (3.3) takes on the form

$$f_\infty(x) = \int_0^\epsilon \mathrm{d}y g(y) \ln\left[(\Delta x - cy)^2 + y^2\right] + \ldots, \tag{3.4}$$

where $\Delta x = x - x_\mathrm{c}$ and $g(y)$ is the density of zeros on the line $\xi(y) = x_\mathrm{c} + cy + \mathrm{i}y$ (for $y < \epsilon \ll 1$). The dots denote the contribution from the remaining zeros, lying further away from the critical point. Taking the derivative of both sides and changing the integration variable from y to $w = y/|\Delta x|$, we obtain

$$f'_\infty(x) = \int_0^{\epsilon/|\Delta x|} \mathrm{d}w g\left(w|\Delta x|\right) \frac{2(-cw \pm 1)}{(cw \pm 1)^2 + w^2} + \ldots, \tag{3.5}$$

where the signs $\pm$ correspond to $x = x_\mathrm{c} \pm |\Delta x|$. When the density of zeros on the curve approaches a finite constant $g(y) \to g_0 > 0$ for $y \to 0$, then the integrals (3.5) on both sides of x_c may take on different values, leading to a discontinuity of $f'_\infty(x)$ at $x = x_\mathrm{c}$, and a first order phase transition. One can show that in this case zeros approach the critical point perpendicularly to the real axis [22], meaning that the coefficient c in equation (3.5) equals zero. If $g(y) \to 0$ for $y \to 0$, then the discontinuity of the first derivative disappears, but higher derivatives may have a discontinuity or a divergence at the critical point. In particular, when the density behaves as $g(y) \sim y^{1-p}$ for $y \to 0$, where $p \in (0, 1)$ then the contribution from the integral in (3.5) tends to zero as $f'_\infty(x) \sim |\Delta x|^{1-p}$, but the next derivative diverges

$$f''_\infty(x) \sim |\Delta x|^{-p}, \tag{3.6}$$

so the transition is second order. The grand-canonical thermodynamic potential $\psi(\mu)$ is directly related to $f_\infty(x)$: $\psi(\mu) = f_\infty(\mathrm{e}^{-\mu})$. This means, in particular, that the divergence of $f''_\infty(x)$ for $x \to x_\mathrm{c}^+$ leads to a divergence of $\psi''(\mu)$ for $\mu \to \mu_\mathrm{c}^-$ with the same exponent p

$$\psi''(\mu) \sim (\mu_c - \mu)^{-p}. \tag{3.7}$$

Comparing the last equation with (2.10), we see that for the zeta-urn model

$$p = \lambda = 2 - \frac{1}{\beta - 1}. \tag{3.8}$$

The exponent describing the divergence of the second derivative of the grand-canonical thermodynamic potential is thus directly related to the exponent describing the behaviour of the density of zeros on the curve near the critical point ($y \to 0$)

$$g(y) \sim y^{1-p}, \tag{3.9}$$

or equivalently to the exponent of the cumulative density function $G(y) = \int_0^y g(y')\mathrm{d}y'$

$$G(y) \sim y^{2-p}. \tag{3.10}$$

The cumulative density $G(y)$ can be reconstructed from its counterpart $G_S(y)$ for finite S, by sending S to infinity $G(z) = G_\infty(z) \equiv \lim_{S\to\infty} G_S(z)$. Let $z_j = x_j + \mathrm{i}y_j$ be the loci of zeros for finite S. The index j goes from 1 to S. The zeros z_j in the upper half plane are indexed in order of increasing distance $|z_j - x_\mathrm{c}|$ from the critical point. If the first zeros indeed lie on a smooth curve, then the imaginary parts are also ordered $y_1 \leqslant y_2 \leqslant y_3 \ldots$, $j = 1, 2, \ldots,$. The conjugate zeros which are located symmetrically in the lower plane can also be ordered, for example $z_{S+1-j} = \bar{z}_j = x_j - \mathrm{i}y_j$, but the way they are ordered is inessential for the calculation which concentrates on the first zero in the upper half plane. The cumulative density for the first zeros is:

$$G_S(y_j) = \frac{j}{S}, \tag{3.11}$$

because the right-hand side gives the fraction of all zeros which lie near the critical point and whose imaginary part $y \in [0, y_j]$. Generally, $G_S(y)$ is a staircase function with steps of height $1/S$ which decrease to zero when S tends to infinity. For large S, the function $G_S(y)$ should approach the limiting distribution (3.10), so for large S we can expect that the zeros must scale as

$$y_j \sim \left(\frac{j}{S}\right)^{\frac{1}{2-p}}, \tag{3.12}$$

in order to correctly reproduce the right-hand side of (3.11) for large S. In other words, we see that the phase transition properties are encoded in the scaling of the loci of zeros closest to the critical point. In particular, we see that for $y_j \sim j$ for $p = 1$, so the zeros are equidistant. For $p = 0$, which is a marginal value for the transitions of second and third order, the last formula gives $y_j \sim j^{1/2}$. For the zeta-urn model, equations (3.10) and (3.12) translate to

$$G(y) \sim y\,, \quad y_j \sim \frac{j}{S}, \tag{3.13}$$

for $\beta \in [2, +\infty)$, where the transition is first order, and

$$G(y) \sim y^{\frac{1}{\beta-1}}\,, \quad y_j \sim \left(\frac{j}{S}\right)^{\beta-1}, \tag{3.14}$$

for $\beta \in [3/2, 2)$ (3.8), where the transition is second order. What happens for $\beta \in (1, 3/2)$, where the transition is higher order, requires a further discussion. The expression on the left-hand side of (3.7) corresponds to normalised variance of N

$$\psi''(\mu) = \lim_{S\to\infty} \frac{\langle N^2\rangle_{S,\mu} - \langle N\rangle_{S,\mu}^2}{S} = \lim_{S\to\infty} \frac{\sigma^2_{S,\mu}(N)}{S} \tag{3.15}$$

as directly follows from the definition (2.8). In the fluid phase, for a given $\mu < \mu_\mathrm{c}$, the fluctuations of N grow as a square root of S: $\sigma_{S,\mu}(N) \sim \sqrt{S}$, so the normalised variance tends to a constant, $\psi''(\mu)$, as S tends to infinity. For the first and second order phase transitions, at the critical point $\mu \to \mu_\mathrm{c}$, the fluctuations grow faster than $\sqrt{S}$ leading to the divergence of $\psi''(\mu)$ in the limit $S \to \infty$ (3.15). For the third or higher order phase transition, however, the fluctuations at the critical point behave asymptotically as $\sigma_{S,\mu}(N) = \sigma_\mathrm{c}\sqrt{S} + o(\sqrt{S})$. If the coefficient σ_c is non-zero, then the normalised variance (3.15) tends to a positive constant $\psi''(\mu_\mathrm{c}) = \sigma_\mathrm{c} > 0$ at the critical point. In this case, $p = 0$, as can be seen from (3.7). If in turn the leading term vanishes, $\sigma_\mathrm{c} = 0$, then $\psi''(\mu_\mathrm{c})$ tends to zero and as a consequence the exponent p (3.7) takes on a negative value, which is the case for the zeta-urn model. More generally, one can show [2] that all derivatives $\psi^{(k)}(\mu_\mathrm{c}) = 0$, for $k = 1, \ldots, n$, vanish at the critical point for $\beta \in [1 + 1/(n+1), 1 + 1/n)$, and, as a consequence, the scaling relations (3.14) apply to the entire range $\beta \in (1, 2)$, where the phase transition is second or higher order.

4. Finite size analysis

For moderate system sizes, up to S of the order a thousand, computations of the partition function for the zeta-urn model (2.1) can be done directly by algebraic calculations. The procedure is straightforward. We first specify β, hence fixing the order of the transition, and S, and then evaluate $Z_{S,N}$'s for the requisite $N = 1, \ldots, S$ using the recursion relation of (2.2). The roots of the polynomial

$$Z_S(z) = \sum_{N=1}^{S} z^N Z_{S,N}, \tag{4.1}$$

are then extracted to obtain the partition function zeros in the complex $z = \exp(-\mu)$ plane. We performed computations for sizes up to $S = 2000$, using Mathematica®.

To estimate $G(y)$, we select the zeros nearest to the critical point in the upper half-plane and fit the function

$$G(y) = ay^b + c, \tag{4.2}$$

with three parameters a, b, c to the data points $(y_j, (j - 1/2)/S)$, $j = 1, \ldots, n$ (3.11) for the first n zeros [31]. The parameter c is a finite size correction, which is expected to tend to zero when S tends to infinity. From the exponent b we can estimate $p = 2 - b$. For first order phase transitions $b = 1$, while for higher order transitions $b = 1/(\beta - 1)$.

We can also estimate the exponent directly from the positions of the first zeros (3.12). In the analysis we should take into account possible finite size corrections. The simplest finite size corrections to (3.12) have the form

$$y_j = \left(\frac{j + c}{aS + b}\right)^d, \tag{4.3}$$

where $d = 1/(2 - p)$, and a, b, c are real parameters representing finite size corrections to (3.12). We have used the same letters here as in (4.2) but now they have a different meaning. This formula can be applied with a free parameter d which can be fitted from the data and then can be used to estimate the exponent p. Alternatively, the value of d can be fixed theoretically, to check whether the theoretical prediction describes the data well. In this case, only a, b and c are fitted. We will take the latter approach here, setting $d = 1$ for $\beta \in [2, +\infty)$ and $d = \beta - 1$ for $\beta \in (1, 2)$ according to the theoretical predictions.

5. Results

5.1. First order regime

As an example we take $\beta = 9/2$, where the transition is well into the first order regime ($\beta > 2$). The expectation is that the zeros will impact the positive real axis in the complex fugacity plane at the pseudo-critical point $z_{\rm pc}(S)$, which will tend to the critical point $z_{\rm c}(S) = \exp(-\mu_{\rm c}) = 1/\zeta(\beta)$ for $S \to \infty$. For $\beta = 9/2$, $z_{\rm c} = 1/\zeta(9/2) \approx 0.94813$. The change of the position of the pseudo-critical point with S can be seen in figure 1(a) where the zeros are plotted for $S = 600$ and $S = 2000$. In figure 1(b) we show the best fit $G(y) = ay^b + c$ (4.2) to $n = 20$ first zeros. The best fit gives the power $b = 1.032$ and $b = 1.028$ for $S = 600$ and $S = 2000$, respectively, exhibiting a tendency to move towards $b = 1$, expected for a first order transition. The fitted value of c (4.2) is $c = -1.6 \cdot 10^{-5}$ and $-0.7 \cdot 10^{-5}$ for $S = 600$ and $S = 2000$, so it tends to zero with increasing S, as expected. An alternative check of the scaling of first zeros, expected for the first order phase transition, is to use (4.3) with $d = 1$. As shown in figure 2) the scaling formula (4.3) very well reproduces the dependence $y_j(S)$ both as function of j and S.

Another property that we can check from the distribution of the zeros in the first order case is magnitude of the discontinuity in $\psi'(\mu)$ at $\mu_{\rm c}$, which is given theoretically from the saddle point solution as $\Delta\psi'(\mu_{\rm c}) = \zeta(\beta)/\zeta(\beta - 1)$ [2]. For $\beta = 9/2$, the numerical value of this discontinuity is $\Delta\psi'(\mu_{\rm c}) \approx 0.93608$. On the other hand, this value is related to the position of the first zero [18, 19], or equivalently to the parameter a (4.2) as $\Delta\psi'(\mu_{\rm c}) \approx 2\pi a$. The numerical value of $2\pi a$ deduced from the partition function zeros for $S = 2000$ is $2\pi \times 0.1687 \approx 1.059$ which is in a moderately good agreement with the saddle point value. One would expect a better agreement for larger S.

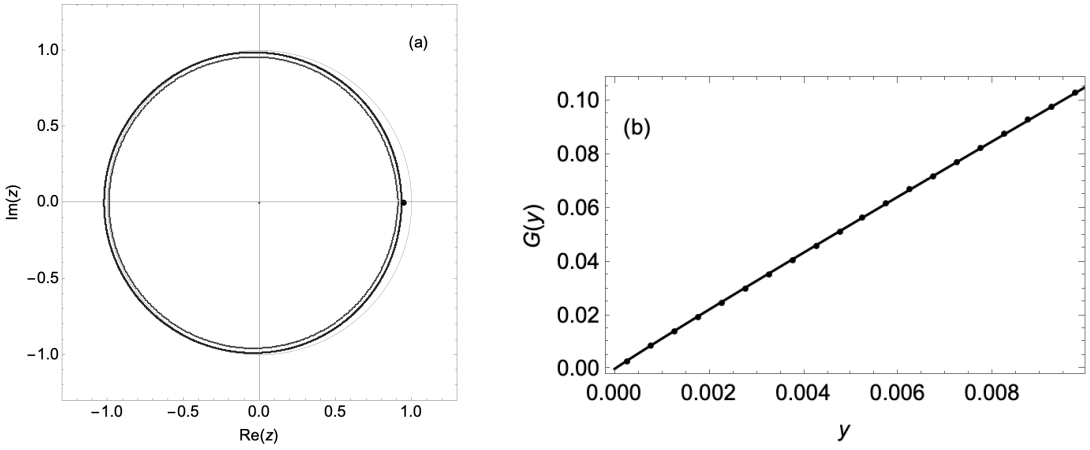

Figure 1. (a) Partition function zeros for $\beta = 9/2$ for $S = 600$ (gray) and $S = 2000$ (black). One can see that the contour on which the zeros lie expands slightly with S. The contours are close to the unit circle which is drawn as thin line. The black point on the real axis at $\exp(-\mu_c) = 1/\zeta(9/2) \simeq 0.94813$ is drawn to highlight that the zeros are impacting the real axis vertically close to the expected (infinite size) critical value. (b) Fitting the cumulative density for the first 20 zeros for $\beta = 9/2$ and $S = 2000$ to $G(y) = ay^b + c$ gives $a = 0.1687(6)$, $b = 1.028(1)$ and $c = -0.7(5) \cdot 10^{-5}$.

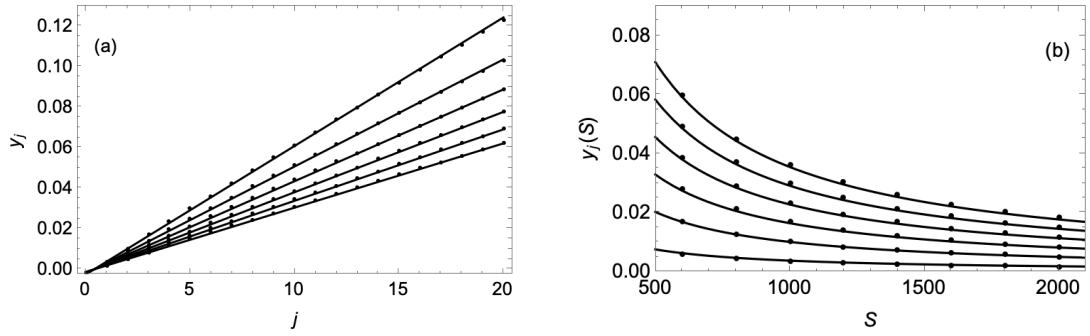

Figure 2. (a) The imaginary parts y_j of the first twenty zeros plotted against j, for $S = 1000, 1200, \ldots, 2000$ from top to bottom. The solid lines are given by (4.3) with $a = 0.1575$, $b = 0$, $c = 5.64$ and $d = 1$. (b) The imaginary parts $y_j(S)$ of the first six zeros plotted against S for $j = 1, 2, \ldots, 6$ from bottom to top. The solid lines are given by (4.3) with the same parameters as in (a).

5.2. Second (and higher) order regime

As $\beta \to 2$ and the strength of the first order transition weakens and the distribution becomes less circular. Since $\psi''(\mu)$ displays a logarithmic singularity at $\beta = 2$ it is not a particularly friendly value for numerical explorations. Out of an abundance of caution we move into the range of β where the transition is second order and does *not* have logarithmic corrections, taking $\beta = 7/4$, which we show in figure 3. From (2.10) this gives a diverging second order phase transition with $\psi''(\mu) \sim (\mu_c - \mu)^{-2/3}$ (2.11) and $G(y) \sim y^{4/3}$ (3.14). The best fit (4.2) produces a value $b = 1.39$ close to the expected one. The fit is shown in figure 3(b). Also the dependence of $y_j(S)$ on j and S is consistent with (4.3) using the power $d = \beta - 1 = 3/4$ as shown in figure 4.

The transition will be n-th order for $\beta \in [1 + 1/n, 1/(n-1))$. The general form of the locus of zeros does not change as $\beta \to 1$, though the pinch point on the real axis tends to the origin, $z_c \to 0$, as $\mu_c \to \infty$. We will present a quantitative investigation of the higher order scaling elsewhere. As mentioned, the *ansatz* $G(y) \sim y^{1/(\beta-1)}$ appears to extend to the higher order transition region for the entire range $\beta \in (1, 2)$ but for $\beta \in (1, 3/2]$ it is difficult to discern using a finite size scaling analysis because it is overshadowed by the behaviour $G(y) \sim y^2$ coming from the maximum of the second derivative, which lies very close to the critical point.

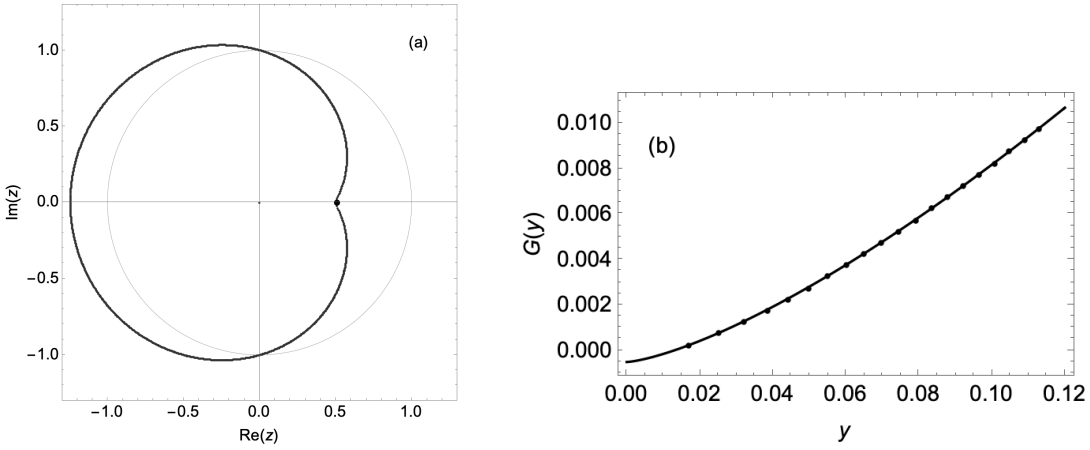

Figure 3. (a) Partition function zeros for $\beta = 7/4$ and $S = 1200$. The unit circle as reference is drawn with a thin line. The critical point is drawn as a black point on the real axis at $\exp(-\mu_c) = 1/\zeta(7/4) = 0.50960$. The line going through the smallest zeros hits the real axis at a pseudo-critical point which is slightly away from the critical point. The pseudo-critical point moves towards the critical point as S is increased. (b) Fitting the cumulative density for the first 20 zeros for $\beta = 7/4$ and $S = 2000$ to $G(y) = ay^b + c$ gives $a = 0.213(2)$, $b = 1.390(6)$ and $c = -0.52(2) \cdot 10^{-3}$.

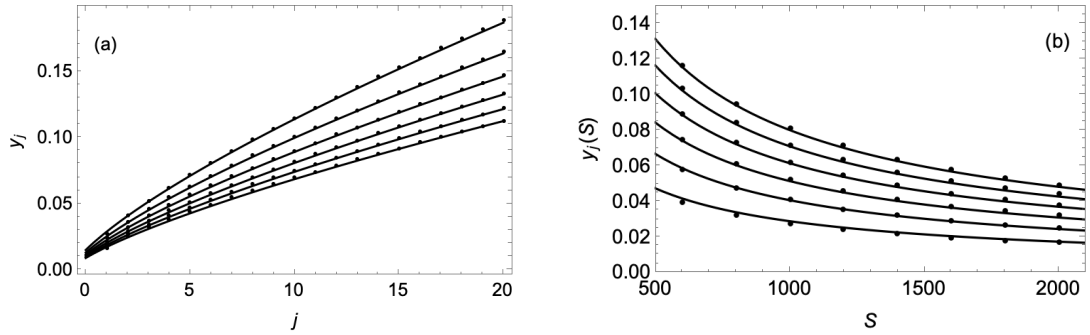

Figure 4. (a) The imaginary parts y_j of the first twenty zeros plotted against j, for $S = 1000, 1200, \ldots, 2000$ from top to bottom. The solid lines are given by (4.3) with $a = 0.73$, $b = 0.1875$, $c = 6.7$ and $d = 3/4$. (b) The imaginary parts $y_j(S)$ of the first six zeros plotted against S for $j = 1, 2, \ldots, 6$ from bottom to top. The solid lines are given by (4.3) with the same parameters as in (a).

5.3. No transition regime

Although the transition vanishes at $\beta = 1$, it is still possible to evaluate the zeros numerically for $0 \leqslant \beta \leqslant 1$ and, indeed, for $\beta < 0$. As expected, the locus of zeros does not impact the (physical) positive real z axis but, nonetheless, still displays interesting behaviour. If we first consider $\beta = 1$, we can see the locus of zeros failing to pinch the real axis in figure 5 (left-hand). As β is reduced further, the locus of zeros moves into the negative half plane as can be seen in figure 5 (right-hand) for $\beta = 1/8$.

It is possible to evaluate $Z_{S,\mu}$ explicitly for $\beta = 0$ which was done in [2], where it was observed that $Z_{S,N} = \binom{S-1}{N-1}$ and the sum in (2.7) was then carried out to give $Z_{S,\mu} = z(1+z)^{S-1}$ (with $z = \exp(-\mu)$). In this case, the locus of zeros degenerates to the single trivial zero at the origin and an $(S-1)$-fold zero at $z = -1$. For $-1 < \beta < 0$, the locus takes on an airfoil-like shape which thins and extends further left as $\beta \to -1$, eventually collapsing onto the negative real axis for $\beta \leqslant -1$ as can be seen in figure 6.

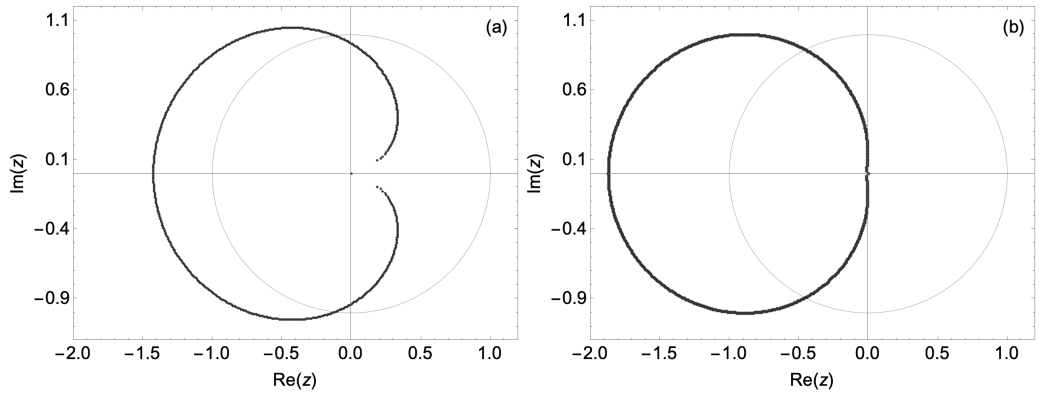

Figure 5. (a) Partition function zeros for $\beta = 1$ and $S = 600$. (b) Partition function zeros for $\beta = 1/8$ and $S = 600$. The unit circle shown for reference is drawn with a thin line.

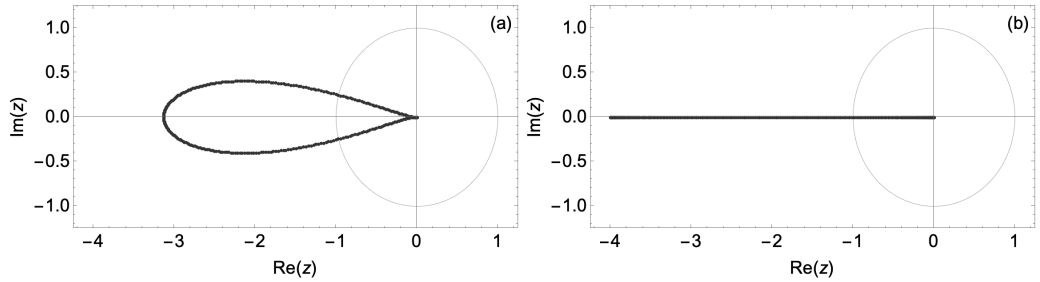

Figure 6. (a) Partition function zeros for $\beta = -3/4$ and $S = 300$. (b) Partition function zeros for $\beta = -1$ and $S = 300$. The unit circle shown for reference is drawn with a thin line.

6. Summary

The analysis of the partition function zeros of the zeta-urn model carried out here has some parallels with that done for the ASEP (asymmetric exclusion process) in [38, 39]. In that case the first and second order nature of the transitions in an ostensibly non-equilibrium model were discernable from "partition function" zeros which were explicitly calculable from the known exact formula for the analogue of the partition function (a steady state normalization). It was later observed that the weights of ASEP configurations could also be regarded as those of an equilibrium model of one transit walks, so the ASEP steady state normalization *was* a standard partition function for this model [40, 41]. Here, the zeta-urn partition function can also be regarded as the non-equilibrium steady state of a zero range process with suitably tuned jump rates. One obvious difference to the ASEP is that transitions of any order are accessible for the zeta-urn here by tuning β, another is that the ensemble considered in the ASEP case was the canonical one.

We have found that the zeta-urn model provides a useful pedagogical illustration of the finite size scaling of partition function zeros for both first order ($\beta > 2$) and continuous ($1 < \beta \leqslant 2$) transitions, by virtue of the relative ease with which the finite size partition functions may be calculated, thanks to (2.2) and (2.7) . Moving away from statistical mechanics, the locus of zeros itself continues to display interesting behaviour for regions in which there is no phase transition (i.e. regions in which the locus does not intersect the positive real axis in the $S \to \infty$ limit). Given that $\psi(\mu)$ is the inverse of a known cumulant generating function, it is tempting to try to find analytical expressions for these curves.

It would also be interesting to devote further numerical resources to exploring the logarithmic corrections at $\beta = 2$ and to use the model to benchmark alternative approaches such as the use of high-order cumulants to extract the scaling of the zeros [42, 43].

Acknowledgments

Ralph Kenna contributed greatly to DAJ's understanding of partition function zeros and finite size scaling, through joint work such as [31, 41] and elsewhere. He will be sadly missed.

References

1. Bialas P., Burda Z., Johnston D., Nucl. Phys. B, 1997, **493**, 505–516, doi:10.1016/S0550-3213(97)00192-2.
2. Bialas P., Burda Z., Johnston D., Phys. Rev. E, 2023, **108**, 064107, doi:10.1103/PhysRevE.108.064107.
3. Drouffe J.-M., Godrèche C., Camia F., J. Phys. A: Math. Gen., 1998, **31**, L19, doi:10.1088/0305-4470/31/1/003.
4. Bialas P., Burda Z., Johnston D., Nucl. Phys. B, 1999, **542**, 413–424, doi:10.1016/S0550-3213(98)00842-6.
5. Godrèche C., Lect. Notes Phys., 2007, **716**, 261–294, doi:10.1007/3-540-69684-9_6.
6. Evans M. R., Braz. J. Phys., 2000, **30**, 42–57, doi:10.1590/S0103-97332000000100005.
7. Evans M. R., Hanney T., J. Phys. A: Math. Gen., 2005, **38**, R195, doi:10.1088/0305-4470/38/19/R01.
8. Grosskinsky S., Schütz G. M., Spohn H., J. Stat. Phys., 2003, **113**, 389-410, doi:10.1023/A:1026008532442.
9. Godréche C., Luck J. M., J. Phys. A: Math. Gen., 2005, **38**, 7215, doi:10.1088/0305-4470/38/33/002.
10. Waclaw B., Bogacz L., Burda Z., Janke W., Phys. Rev. E, 2007, **76**, 046114, doi:10.1103/PhysRevE.76.046114.
11. Majumdar S. N., Evans M. R., Zia R. K. P., Phys. Rev. Lett., 2005, **94**, 180601, doi:10.1103/PhysRevLett.94.180601.
12. Evans M. R., Majumdar S. N., Zia R. K. P., J. Stat. Phys., 2006, **123**, 357–390, doi:10.1007/s10955-006-9046-6.
13. Evans M. R., Majumdar S. N., Zia R. K. P., J. Phys. A: Math. Gen., 2006, **39**, 4859, doi:10.1088/0305-4470/39/18/006.
14. Janson S., Probab. Surveys, 2012, **9**, 103–252, doi:10.1214/11-PS188.
15. Bialas P., Burda Z., Phys. Lett. B, 1996, **384**, 75–80, doi:10.1016/0370-2693(96)00795-2.
16. Bialas P., Burda Z., Waclaw B., AIP Conf. Proc., 2005, **776**, 14–28, doi:10.1063/1.1985374.
17. Godrèche C., J. Phys. A: Math. Theor., 2017, **50**, 195003, doi:10.1088/1751-8121/aa6a6e.
18. Yang C. N., Lee T. D., Phys. Rev., 1952, **87**, 404, doi:10.1103/PhysRev.87.404.
19. Yang C. N., Lee T. D., Phys. Rev., 1952, **87**, 410, doi:10.1103/PhysRev.87.410.
20. Fisher M. E., In: Lecture in Theoretical Physics, Vol. VIIC, Brittin W. E. (Ed.), Gordon and Breach, New York, 1968, 1.
21. Bena I., Droz M., Lipowski A., Int. J. Mod. Phys. B, 2005, **19**, 4269–4329, doi:10.1142/S0217979205032759.
22. Grossmann S., Resenhauer W., Z. Phys., 1967, **207**, 138–152, doi:10.1007/BF01326224.
23. Abe R., Prog. Theor. Phys., 1967, **37**, 1070–1079, doi:10.1143/PTP.37.1070.
24. Abe R., Prog. Theor. Phys., 1967, **38**, 72–80, doi:10.1143/PTP.38.72.
25. Abe R., Prog. Theor. Phys., 1967, **38**, 322–331, doi:10.1143/PTP.38.322.
26. Abe R., Prog. Theor. Phys., 1967, **38**, 568–575, doi:10.1143/PTP.38.568.
27. Suzuki M., Prog. Theor. Phys., 1967, **38**, 289–290, doi:10.1143/PTP.38.289.
28. Suzuki M., Prog. Theor. Phys., 1967, **38**, 1225–1242, doi:10.1143/PTP.38.1225.
29. Suzuki M., Prog. Theor. Phys., 1967, **38**, 1243–1251, doi:10.1143/PTP.38.1243.
30. Suzuki M., Prog. Theor. Phys., 1968, **39**, 349–364, doi:10.1143/PTP.39.349.
31. Janke W., Johnston D. A., Kenna R., Nucl. Phys. B, 2006, **736**, 319–328, doi:10.1016/j.nuclphysb.2005.12.013.
32. Ferrari P. A., Landim C., Sisko V. V., J. Stat. Phys., 2007, **128**, 1153-1158, doi:10.1007/s10955-007-9356-3.
33. Chleboun P., Grosskinsky S., J. Stat. Phys., 2010, **140**, 846–872, doi:10.1007/s10955-010-0017-6.
34. Armendariz I., Grosskinsky S., Loulakis M., Stochastic Processes Appl., 2013, **123**, 3466–3496, doi:10.1016/j.spa.2013.04.021.
35. Chleboun P., Grosskinsky S., J. Stat. Phys., 2014, **154**, 432–465, doi:10.1007/s10955-013-0844-3.
36. Jatuviriyapornchai W., Chleboun P., Grosskinsky S., J. Stat. Phys., 2020, **178**, 682–710, doi:10.1007/s10955-019-02451-9.
37. Godrèche C., J. Stat. Phys., 2021, **182**, 13, doi:10.1007/s10955-020-02679-w.
38. Blythe R. A., Evans M. R., Phys. Rev. Lett., 2002, **89**, 080601, doi:10.1103/PhysRevLett.89.080601.
39. Blythe R. A., Evans M. R., Braz. J. Phys., 2003, **33**, 464, doi:10.1590/S0103-97332003000300008.
40. Blythe R. A., Janke W., Johnston D. A., Kenna R., J. Stat. Mech., 2004, P06001, doi:10.1088/1742-5468/2004/06/P06001.
41. Blythe R. A., Janke W., Johnston D. A., Kenna R., J. Stat. Mech., 2004, P10007, doi:10.1088/1742-5468/2004/10/P10007.
42. Deger A., Brange F., Flindt C., Phys. Rev. B, 2020, **102**, 174418, doi:10.1103/PhysRevB.102.174418.
43. Vecsei P. M., Lado J. L., Flindt C., Phys. Rev. B, 2022, **106**, 054402, doi:10.1103/PhysRevB.106.054402.

Нулі статистичної суми моделі дзета-урн

П. Б’ялас[1], З. Бурда[2], Д. А. Джонстон[3]

[1] Інститут прикладної інформатики Ягеллонського університету, вул. Лоясієвіча 11, 30-348 Краків, Польща

[2] Гірничо-металургійна академія, Факультет фізики та прикладної інформатики, алея Міцкевича 30, 30-059 Краків, Польща

[3] Школа математики та комп’ютерних наук, Університет Геріот-Ватт, Ріккартон, Единбург EH14 4AS, Великобританія

Обговорюється розподіл нулів статистичної суми для великого канонічного ансамблю у моделі дзета-урн, де налаштування одного параметра може дати конденсаційний перехід першого чи будь-якого вищого порядку. Обчислюється геометричне місце нулів для систем скінченого розміру та перевіряються масштабні співвідношення, що описують накопичення нулів поблизу критичної точки у порівнянні з теоретичними передбаченнями як для перехідних режимів першого, так і вищих порядків.

Ключові слова: *Нулі Лі-Янга та Фішера, критичні показники, фазові переходи першого та другого роду*